5-19-2016

Functional Analysis of Wild-Type LGN and T450 Mutants

Ryan Elnicki
The College of New Rochelle, elnickirj@gmail.com

Functional Analysis of Wild-Type LGN and T450 Mutants

A Senior Honors Thesis

Submitted in Partial Fulfillment of the Requirements for Graduation in the Honors College

By:

Ryan J. Elnicki

Biochemistry Major

The College at Brockport

May 19th, 2016

Thesis Director: Dr. Brandy Sreenilayam, Assistant Professor, Department of Chemistry & Biochemistry

Abstract:

The protein LGN, named for the many repeats of the amino acids leucine (L), glycine (G) and asparagine (N), is crucial for mammalian cellular division. Specifically, LGN plays a significant role in cell polarity and alignment of the mitotic spindles and in its absence, the organism ceases to develop. In breast cancer, LGN is upregulated due to phosphorylation of T450 and the knockdown of LGN activity has been shown to suppress growth of breast cancer cells. Furthermore, a mutation to alanine at the 450^{th} position also suppressed breast cancer cell growth. The goal of this project was to explore the biochemistry of both wild-type LGN and two T450 mutants of LGN in hope of gaining insight as to how LGN phosphorylation proliferates cancer. LGN was transiently expressed in BHK-570 tissue culture cells using a pCMV-LGN plasmid and LipoD 293 reagent. Protein expression of wild-type LGN was confirmed by both Western blot and immunocytochemistry of fixed, permeabilized cells using anti-GPSM2 antibody. Furthermore, the T450A and T450D mutants, which mimic the unphosphorylated and phosphorylated forms of LGN respectively, are being generated by PCR and will be sent for sequencing analysis to confirm the completed mutagenesis. Future experiments will determine the effect of phosphorylation of T450 on LGN function; specifically, additional localization studies of T450A and T450D mutants will be conducted and compared to that of wild-type LGN. Characterization of LGN function relative to the phosphorylation status of T450 could lead to the development of novel treatments for breast cancer.

Introduction:

LGN was first identified in 1996 (1) and was designated as LGN due to the presence of 10 Leu-Gly-Asn repeats in the N-terminal half of the protein and was initially classified as a mosaic protein with two distinct domains. The N-terminal domain consists of seven tetratricopeptide repeats (TPR) motifs which can bind to a wide range of protein targets, including NuMA (2,3,4,5). The C-terminal domain contains 4 GoLoco motifs, also known as GPR domains, which can bind various $G_{\alpha i}$ subunits in G-protein regulatory mechanisms (1,6). LGN is known to have an estimated molecular mass of 76 kDa (1), have a basal pI of 6.49 (7), and be expressed in a variety of tissue types including: throughout brain tissue, heart, lung, liver, pancreas, spleen, kidney, testis, ovary, and skeletal muscle (1,8). LGN's official name as approved by HUGO Gene Nomenclature Committee is G-Protein Signaling Modulator 2 (GPSM2). Some of LGN's homologs in various organisms including: Pins in drosophila, AGS5 in *S. cerevisiae*, and GPR1/2 in *C. elegans*. Furthermore, LGN's direct binding partners have their own homologs such as NuMA's homolog Mud in drosophila (4) and Lin-5 in *C. elegans* (9).

LGN was first identified based on its binding interactions with $G_{\alpha i}$ subunits at the protein's GoLoco motifs, specifically the $G_{\alpha i2}$ subunit (1). LGN can bind up to four $G_{\alpha i}$ subunits, one at each GoLoco motifs. Further studies on the selectivity of LGN's GoLoco motifs revealed that all four domains have a high affinity for $G_{\alpha i1}$, $G_{\alpha i2}$, and $G_{\alpha i3}$ but not for $G_{\alpha o}$ subunits (6). Furthermore, these GoLoco motifs act as guanine nucleotide dissociation inhibitors on the $G_{\alpha i}$ subunits, maintaining the $G_{\alpha i}$-GDP complex. The interaction of LGN with $G_{\alpha i}$-GDP to stabilize the $G_{\alpha i}$-GDP complex prevents the reassociation of $G_{\alpha i}$ to $G_{\beta\gamma}$ and allows for $G_{\beta\gamma}$ subunits to continue to stimulate downstream signaling (10). To localize LGN at the cell cortex, G_{α} subunits must be able to interact with the cortical membrane. Myristoylation of G_{α} subunits can tether them to the cell membrane to enrich the presence of LGN to their location (11). Furthermore, actin filaments function to anchor and stabilize the presence of $G_{\alpha i}$ subunits at the cell cortex (12). G_{α} subunits at the cell cortex are essential for the generation of the proper pulling forces by the LGN/NuMA/Dynein complex and the extent of these pulling forces is dependent upon G_{α} activity (Figure 1) (11,12). The Ezrin/Radixin/Moesin complex functions to organize F-actin structures at the cell cortex during metaphase in order to regulate the localization of G_{α} and to allow the recruitment of LGN and NuMA to the cortex (13). During prophase and metaphase, $G_{\alpha i}$ subunits are localized at both the cell cortex and the spindle poles to direct spindle pole polarity and positioning for cell division (14).

During interphase, NuMA is localized at the nucleus as part of the nuclear transport machinery and nuclear scaffold, however, upon initiation of mitosis and the breakdown of the nuclear envelope, LGN will recruit NuMA to the cell cortex (15,16). When bound to LGN, amino acids 1878-1910 of NuMA will occupy all of the seven TRP motifs of LGN (17). When not bound to LGN, NuMA will bind to and stabilize the minus ends of astral microtubules through amino acids 1900-1971 to promote their formation for proper orientation of the mitotic spindles. Due to the 10 amino acid overlapping binding sites on NuMA, the latter interaction can be disrupted by LGN binding to NuMA and subsequently suppress astral microtubule formation (2,18,19). Further research revealed an alternate microtubule binding domain at amino acids 2002-2115 which allow for simultaneous interactions with both LGN and astral microtubules to maintain microtubule orientation towards the cell poles (20). During mitosis, NuMA colocalizes with LGN at the spindle poles as well as the cell cortex as part of the $G_{\alpha i}$/LGN/NuMA complex (18). However, it was determined in HeLa cells that NuMA's localization at the apical cortex during metaphase depended on both LGN presence in the apical cortex and the phosphorylation of Y1774 of

NuMA, which is regulated by the kinase ABL1 (21). In order to generate pulling forces on astral microtubules, NuMA in the $G_{\alpha i}$/LGN/NuMA complex recruits dynein/dynactin to provide plus-end pulling forces on the astral microtubules which works to orient the mitotic spindles and direct cell polarity (Figure 1) (22,23). These pulling forces on the astral microtubules function to anchor the microtubules at the cell cortex (24) and properly position the microtubules and spindle poles for cell division (25). Spindle pole orientation dictates partitioning of cells during mitosis and fate of daughter cells after mitosis is completed (26).

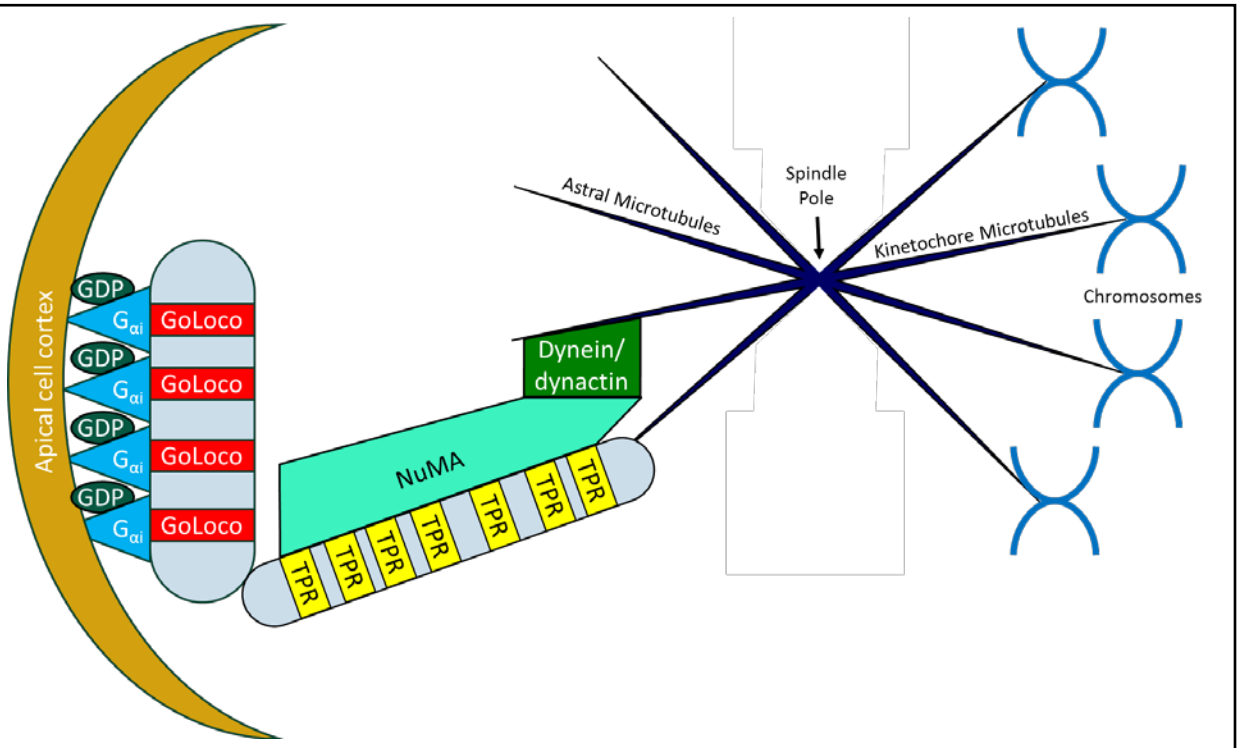

Figure 1: Schematic diagram of protein assembly for force generation and pulling on astral microtubules and ultimately one of the sister chromatids during metaphase of mitosis.

LGN is found to be expressed throughout the cell cycle but its highest expression is during the G2 phase and mitosis (27) where it tends to localize at the spindle poles and cell cortex during metaphase and at the midline during cytokinesis (14). Specifically, LGN functions to direct cell polarity and orient the mitotic spindles during cell division. This is achieved through a series of regulatory steps which work to recruit LGN to the cell cortex, activate LGN, allowing LGN to influence further proteins for the regulation of mitotic spindles. In mammalian cells, par3/par6/aPKC complexes recruit LGN to the cell cortex through the binding of the adapter protein mInsc to LGN (4,15). Similarly, in drosophila, the Baz/Par-6/aPKC/Insc complex recruits Pins to the apical cortex at late interphase, allowing Pins to subsequently bind to $G_{\alpha i}$, which is consistent with the Par-3/mInsc interactions with LGN in mammalian systems (17). In Chinese Hamster Ovary cells, LGN colocalizes with $G_{\alpha i3}$ at the cell cortex during metaphase as well as at the spindle poles in order to direct cell polarity (14). At the apical cortex, aPKC phosphorylates LGN at S401 which allows for binding of LGN to a 14-3-3 protein, dissociating LGN from Gαi (15). This regulation results in an inhibition of LGN orientation activity. LGN activity is also regulated by the protein Ric-8a which can enzymatically dissociate the $G_{\alpha i}$-GDP/GoLoco interactions by activating $G_{\alpha i}$ through the exchange of a GTP molecule for the bound GDP and subsequently causing the release of NuMA from

LGN to regulate the pulling force of microtubules during mitosis (28). Another form of regulation for LGN is an autoinhibition self-regulation. In cells, LGN is a conformational switch which will form an autoinhibited structure where the N- and C-terminal domains of LGN will interact with each other (18,29). Specifically, GoLoco motifs 1 and 2 along with GoLoco motifs 3 and 4 will from interactions with TRP motifs 0-3 and 4-7, respectively (30). The mechanism leading to the release of this structure and binding to $G_{\alpha i}$ and NuMA is disputed. Some theories state that LGN will first bind to Gαi in the cortical poles, releasing the autoinhibited form of LGN allowing for TPR motifs to then bind NuMA (30,31). However, at least one report suggests that NuMA will initially bind to LGN, releasing the closed conformation of LGN thus allowing for subsequent binding of LGN to $G_{\alpha i}$ at the cortical positions (18). Regardless of order, the binding of either $G_{\alpha i}$ or NuMA to LGN releases the GoLoco-TPR interactions and allows for cooperative binding of both proteins to LGN. In the end, LGN function must be tightly controlled to ensure that proper planar divisions occur during development and cells divide evenly (32).

LGN protein has been found to be upregulated in various forms of breast cancer and is believed to be a critical factor in the overactive mitosis of the cancer cells (27). LGN knockdown by siRNAs halted cell division and prevented the completion of mitosis. It was demonstrated that phosphorylation of T450 caused the upregulation through the mutagenesis of T450 to A450 (T450A). This T450A mutant LGN induced growth suppression and abnormal chromosomal segregation in breast cancer cells. These effects show a potential target to suppress the proliferation of breast cancer. Our research sets out to characterize the functions on LGN during the cell cycle in regards to the phosphorylation status of T450. This will be done by comparing localization patterns of wild-type LGN to T450A and T450D LGN. These mutants have been selected due to their simulation of a potential phosphorylation at the 450^{th} amino acid site. The T450A mutant will mimic the lack of phosphorylation whereas the T450D will simulate the presence of phosphorylation at T450. To supplement our research on LGN function, LGN protein isolation, purification, and crystallography is also being performed in order to determine the 3D crystal structure of LGN and the T450 mutants. Understanding the functions and structures of wild-type LGN and the T450 mutants will allow us to understand the effects that T450 phosphorylation have on the regulation of LGN activity. Further understanding of this regulatory activity could lead to the development of breast cancer treatments which block the activation of LGN and prevent proliferation of cancer cells.

Materials and Methods:

Cells, plasmids, and antibodies

XL1-Blue supercompetent cells and BL21(DE3) competent cells were purchased from Agilent Technologies. Top10 competent cells were purchased from Invitrogen Life Technologies. DH5α cells were purchased from Fisher Scientific. BHK-570 cells were kindly donated by Dr. Cook from The College at Brockport.

pET-28a—LGN was kindly donated by Nikolai O. Artemyev at the University of Iowa. pET-15b—LGN was purchased from GenScript. pCMV—LGN was purchased from OriGene.

Rabbit anti-His_6 antibody was purchased from GenScript. Rabbit anti-GPSM2 antibody and goat anti-rabbit HRP-conjugated antibody were purchased from Fisher Scientific.

LGN Expression and Purification in *E. coli*

E. coli cells were grown in 1 L of 2xYT media at 37 °C and 250 rpm in the presence of the proper antibiotic for either the pET-28a or pET-15b plasmid (50 μg/mL of kanamycin or 0.14 nM ampicillin, respectively). When the cells reached an OD_{600} of 0.5-0.75, the cells were induced to express LGN by isopropyl β-D-1-thiogalactopyranoside (IPTG) (50 or 250 μM). After 16 hours, the cells were centrifuged at 7,000 rpm and 4 °C for 10 minutes. The pellet was stored at -20 °C until later.

LGN was isolated by resuspending cells in 50 mL of the proper chromatography binding buffer (affinity: 150 mM NaCl, 20 mM phosphate buffer (pH 7.3), 20 mM imidazole; anion-exchange: 20 mM phosphate buffer (pH 6.8, 7.3, 7.7, or 8.0) containing 50 mM NaCl and 2 mM β-mercaptoethanol) with one Roche cOmplete ULTRA Tablet (EDTA-free) and then sonicated with a Model 505 Sonic Dismembrator from Fisher Scientific in an ice water bath with varied conditions of 60% amplitude for 5 minutes, 30% amplitude for 5 minutes, 60% amplitude for 2.5 minutes, 40% or 50% amplitude for 2.5 or 3 minutes. The cell solution was centrifuged at 13,000 rpm for 35 min at 4 °C and the pellet was discarded.

The supernatant was loaded onto a HPLC column (Co^{2+} affinity or Mono Q anion-exchange) with a flow rate of 0.5 mL/min. LGN was eluted with 15 mL of the proper elution buffer (affinity: 150 mM NaCl, 20 mM phosphate buffer (pH 7.3), 250 mM imidazole; anion-exchange: 20 mM phosphate buffer (pH 6.8, 7.3, 7.7, or 8.0) containing 250 mM NaCl and 2 mM β-mercaptoethanol). Initially, the samples were concentrated to under 5 mL using Amicon 15-Ultra 10 kDa MWCO tubes.

Fractions were analyzed by SDS-PAGE, followed by coomassie blue staining to determine purity or transferred to a PVDF membrane for Western blot analysis. A Western blot was performed to detect the presence of LGN using either a rabbit anti-His_6 or rabbit anti-GPSM2 primary antibody (1:1,000 dilution) and a goat anti-rabbit HRP-conjugated secondary antibody (1:5,000 dilution). A colorimetric Pierce CN/DAB Substrate kit was used to detect the presence of bands.

Transformation and Plasmid Purification

Heat-shock transformation of Top10 Competent cells was performed according to the protocol from Invitrogen Life Technologies.

Electroporation transformation of DH5α cells was performed according to the protocol from Fisher Scientific.

After transfection, cells were allowed to grow for 1 hour in SOC media then subsequently plated on LB agar plates containing 50 µg/mL of kanamycin or 0.14 nM ampicillin for growth. Colonies were picked and grown in 10 mL of 2xYT media overnight at 37 °C and 250 rpm for protein expression and purification or plasmid isolation.

Maxipreps were preformed according to standard protocols.

Generation of Mammalian LGN Vector Stock

The pCMV—LGN plasmid was purchased and transformed into DH5α cells. It was subsequently isolated by maxi-prep and stored at -20 °C at a concentration of 1 $\frac{mg}{mL}$. This stock of pCMV—LGN plasmid was used for transfection of mammalian cell lines and nested PCR to generate T450 mutant LGN.

LGN Expression in BHK

Cell Growth and Maintenance

BHK-570 cells were grown in DMEM growth media containing 10% FBS at 37 °C and 5% CO_2.

LipoD Transfection

BHK-570 cells were grown to 80% confluency before the transfection protocol was performed. First, the growth media was changed and the pCMV-LGN plasmid and LipoD reagent were mixed with equal volumes of DMEM then were mixed together. After 15-30 minutes of incubation at room temperature, the LipoD—pCMV-LGN solution was added dropwise to the cell culture. Cells were allowed to express LGN protein for 24 hours.

Immunofluorescence

Cells that were adhered to coverslips in 3.5 cm dishes were transfected according to the previously mentioned LipoD transfection protocol. After 18-24 hours of expression, cells were fixed on the coverslips with 4% paraformaldehyde. Coverslips were incubated in blocking buffer (137 mM NaCl, 2.7 mM KCl, 10 mM Na_2HPO_4, 1.8 mM KH_2PO_4, 0.1% Tween-20, 5% goat serum, pH 7.4) for 30 minutes at room temperature. Next, coverslips were incubated overnight at 4 °C with blocking buffer containing 1:1,000 rabbit anti-GPSM2 antibody. Coverslips were washed for 5 minutes with ice cold PBS 3 times and were incubated for 20 minutes at room temperature in blocking buffer containing 1:500 goat anti-rabbit DyLight 488 conjugated antibody and 1:500 DAPI. Protein localization was determined by fluorescent microscopy using a Zeiss AxioSkop with Axiovision Software.

Mutagenesis protocols

QuikChange Site-Directed Mutagenesis

T450A mutagenesis was performed according to Stratagene's QuikChange Site-Directed Mutagenesis Kit manufacturer's instructions in which 2 µL or 4 µL of full-length LGN DNA template (pET-28a—LGN) was used. All mutagenesis products were run on a 1% agarose gel to check for the presence of a plasmid.

The resulting plasmid was transformed into BL21(DE3) competent cells, XL1-Blue supercompetent cells, or Top10 competent cells using the manufacturer's instructions. The transformed cells were plated on LB agar plates containing 50 µg/mL kanamycin. Plates were incubated overnight at 37 °C. Colonies were picked and grown in 10 mL of 2xYT media overnight at 37 °C and 250 rpm. The plasmid was isolated from the cells grown in the 10 mL of 2xYT media by using the GeneJET Plasmid Miniprep kit purchased from Fisher Scientific. The miniprep product was run on a 1% agarose gel to confirm the presence of a plasmid.

Site-Directed Mutagenesis

PCR site-directed mutagenesis was performed based on instructions from Agilent Technologies. Template DNA (pET-15b—LGN) remaining after the PCR reaction was digested with 1 µL of DpnI for 1 hour at 37 °C. Products were run on a 1% agarose gel and extracted using a gel extraction kit from Qiagen or Fisher Scientific.

Nested PCR Mutagenesis

Nested PCR was performed to generate the T450A and T450D mutants using pCMV—LGN. First, two rounds of PCR were performed: the first reaction used a primer at a site upstream of LGN on the template strand and a primer coding for the respective mutation at the T450 site on the non-template strand; the second used a primer at a site downstream of LGN on the non-template strand and a primer coding for the respective mutation at the T450 site on the template strand. Products were run on a 1% agarose gel and extracted using a gel extraction kit purchased from Fisher Scientific. A final PCR is performed using the previously generated segments along with the primer at a site upstream of LGN on the template strand and the primer at a site downstream of LGN on the non-template strand to generate the full length mutant LGN segment. The product was then run on a 1% agarose gel and extracted using a gel extraction kit and ligated into an empty pCMV plasmid using NotI.

Immunoprecipitation

The entire process was performed on ice at 4 °C. Cells were chilled and washed with ice cold PBS. Cells were lysed with lysis buffer (150 mM NaCl, 50 mM Tris (pH 8.0), 1% NP-40, 1 mM EDTA, 1:1,000 protease & nuclease inhibitor cocktail from Sigma Aldrich) and incubated for 5 minutes. Lysates were scraped off of the dish and the solution was transferred to chilled microfuge tubes and incubated for 20 minutes. Microfuge tubes were centrifuged at 13,200 rpm for 10 minutes at 4 °C and the supernatant was decanted to clean, chilled microfuge tubes. One µL of rabbit anti-GPSM2 antibody was added to the solution and incubated overnight at 4 °C with gentle rocking. Eighty µL of protein A/G Plus-Agarose beads were added to the solution and incubated for 1 hour at 4 °C with gentle rocking. The solution was centrifuged at 13,200 rpm for 2 minutes and 4 °C to pellet the beads and the supernatant was decanted. The pellet was resuspended in IP wash buffer (150 mM NaCl, 50 mM Tris (pH 8.0), 0.1% NP-40, 1 mM EDTA) and centrifuged at 13,200 rpm for 2 minutes and 4 °C to pellet the beads; the wash and centrifugation steps were repeated 4 times. During the last wash, the pellet was resuspended and equally distributed into four clean, chilled microfuge tubes. To isolate and purify LGN by itself, GPSM2 peptide (none, 1:100, 1:500 or 1:1,000) that corresponds to the GPSM2 antibody was added to the beads at 4 °C for 16 hours with gentle rocking. The solution was centrifuged at 13,200 rpm for 2 minutes and 4 °C and the supernatant was transferred to a clean microfuge tube. The presence of LGN protein was analyzed by SDS-PAGE and Western blot using the anti-GPSM2 antibody followed by film detection.

Results and Discussion:

Transformation of LGN Vector into *E. coli*

In order to express full length LGN for purification and crystallography, full length LGN vectors were first transformed into *E. coli* cells for protein expression. *E. coli* were chosen as the expression system because they are able to quickly express large amounts of protein. XL1-Blue supercompetent cells, Top 10 competent cells, and DH5α cells were used for efficient transformation and plasmid propagation. BL21(DE3) competent cells were used for efficient protein expression through their expression of the T7 RNA polymerase for transcription of the vectors (Figure 2).

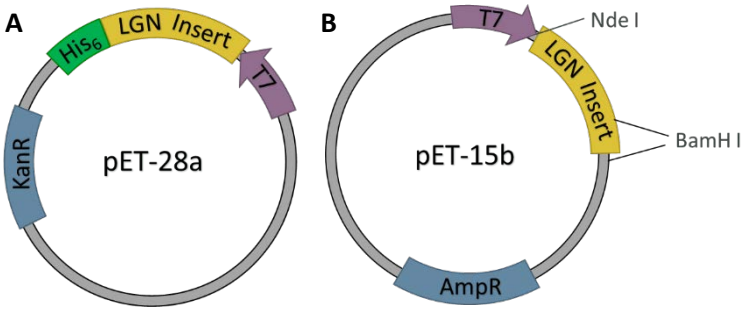

Figure 2: Schematic representation of pET-28a—LGN **(A)** and pET-15b—LGN **(B)**. pET-15b is 5708 bp long and the LGN insert is 2031 bp long.

After the transformation with pET-28a—LGN (Figure 2A) directly into XL1-Blue Supercompetent cells, the cells were grown on LB plates in the presence of kanamycin. The ability of the XL1-Blue supercompetent *E. coli* cells to grow in the presence of kanamycin suggested that a transformation of the pET-28a—LGN plasmid took place. A subsequent isolation of the plasmid from the XL1-Blue Supercompetent cells was performed and then run on a 1% agarose gel to confirm that the transformation was a success but no bands were present in the gel. Further attempts to transform the pET-28a—LGN plasmid into XL1-Blue supercompetent cells were unsuccessful, resulting in only the growth of satellite colonies. Top10 competent cells were purchased for initial plasmid transformation protocols in order to clone and purify a large amount of plasmid for a subsequent transformation into BL21(DE3) competent cells for protein expression via the vector.

Next, the pET-28a—LGN plasmid from the stock was run on a 1% agarose gel and the band at 7500 kb was purified from the gel (Figure 3A). We confirmed that the plasmid was successfully transformed into Top10 cells as indicated by the *E. coli* cells growth on LB agar plates in the presence of the antibiotic kanamycin. Subsequent plasmid isolation from the cultured colonies and analysis of the products by electrophoresis on a 1% agarose gel resulted in an absence of plasmid at 7500 kb (Figure 3B). Although the initial results sugested that a transfromation took place, without confrimation through a subsequnt plasmid isolation it cannot be confimed that the Top10 cells actually contain the pET-28a—LGN plasmid. Without any positive results using the pET-28a—LGN plasmid, we purchased a pET-15b—LGN plasmid to achieve LGN expression in *E. coli*.

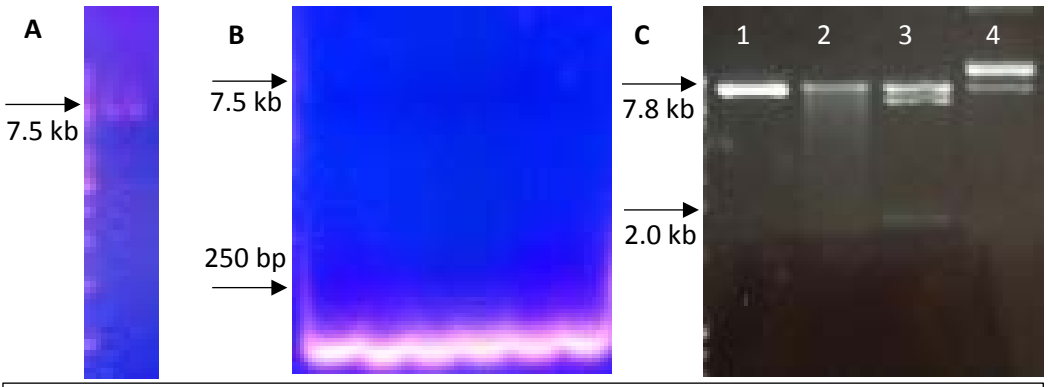

Figure 3: Analysis of the presence of various LGN vectors in *E. coli* cells. **A)** pET-28a—LGN vector from stock at 7500 kb. **B)** Isolation product of pET-28a—LGN from Top10 or Supercompetent cells after transformation, all DNA detected is degraded below 250 bp. **C)** Restriction digest products pf pET-15b—LGN on 1% agarose gel. Lane 1) BamHI, Lane 2) NdeI, Lane 3) BamHI and NdeI, Lane 4) XhoI.

The pET15b—LGN plasmid was transformed into DH5α cells and the cells were grown on LB agar plates containing ampicillin. The vector was subsequently grown in culture, isolated, and verified by restriction digest using BamHI, NdeI, BamHI + NdeI, and XhoI and analysis on a 1% agarose gel (Figures 2B and 3C). Single digests with NdeI and BamHI resulted in the expected band at 7800 bp, the double digest with NdeI and BamHI resulted with two bands at 5700 bp and 2000 bp, and the single digest with XhoI resulted in a supercoiled plasmid structure. These results indicate that the pET-15b—LGN plasmid is present in the DH5α cells and that the LGN is inserted in the correct orientation within the plasmid. A stock of DH5α with pET-15b—LGN in 25% glycerol was stored at -80 °C for future use. pET-15b—LGN was also transformed into BL21(DE3) *E. coli* cells, and expressed LGN when grown in both 2xYT and LB media. Western blot analysis after one round of anion-exchange purification of LGN expression

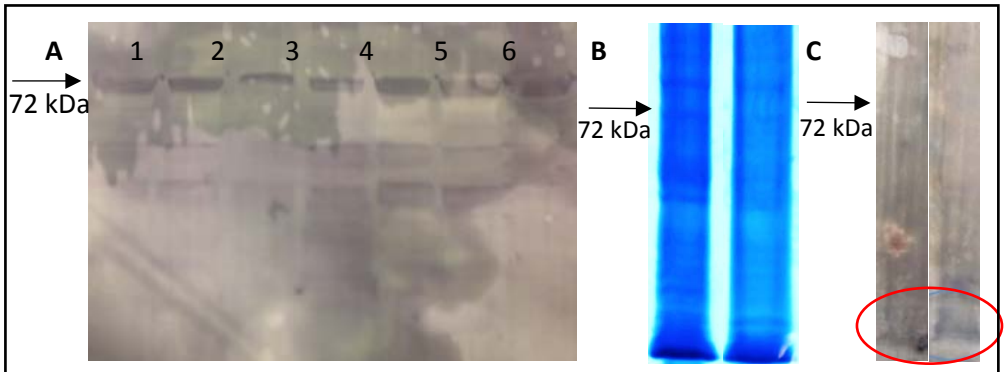

Figure 4: Analysis of LGN expression in *E. coli* cells by coomassie blue stained SDS-PAGE gels and Western blots. **A)** Western Blot after anion-exchange chromatography using anti-GPSM2 antibody. Lane 1) 2xYT Lysate, Lane 2) 2xYT Flow Through and Wash, Lane 3) 2xYT Eluate, Lane 4) 2xYT Pellet Lysate, Lane 5) LB Flow Through and Wash, Lane 6) LB Eluate, Lane 7) LB Pellet Lysate. **B&C)** Two different cell lysates of BL21(DE3) cells after induction of the pET-28a—LGN. **B)** Coomassie blue stained protein gel after affinity chromatography. **C)** Western blot analysis using anti-His_6 primary antibody after affinity chromatography. A faint band appeared near the bottom of the lane as indicated by the red circle.

in BL21(DE3) cells resulted in bands at 75 kDa as expected (Figure 4A). These results indicate that the pET-15b—LGN plasmid is present and viable in the *E. coli* cells. A stock of the *E. coli* with pET-15b—LGN in 25% glycerol was stored at -80 °C for future use. Together, these results indicate that LGN should be able to be readily overexpressed in the *E. coli* cells. This will allow for the development of a scheme to optimize the overexpression and purification of LGN.

LGN Expression in *E. coli* and Purification

In order to purify full length LGN protein, the 25% glycerol stock of pET-28a—LGN transformed into the BL21(DE3) was scraped with a pipet tip and the cells were grown in 2xYT media for LGN expression. After purification of the protein over a Co^{2+} affinity column, a SDS-PAGE gel stained with coomassie blue did not show a band at 75 kDa where LGN is expected to be (Figure 4B). Detection tests for LGN through a Western blot analysis confirmed that there was no presence of LGN (Figure 4C). It was concluded that either transcription or translation for LGN didn't proceed properly or the purification scheme didn't select for LGN. Thus, a different plasmid containing LGN but not a tag was pursued to ensure the tag was not interfering with the ability of LGN to fold correctly in the *E. coli* cells.

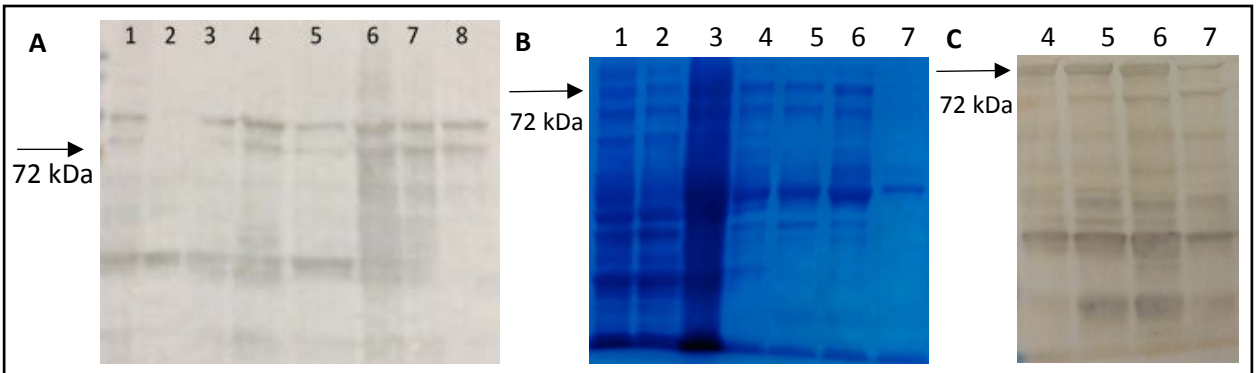

Figure 5: Analysis of sonication effects on LGN stability by coomassie blue stained SDS-PAGE gel and Western blot. **A)** Western blot analysis using anti-GPSM2 primary antibody after anion-exchange chromatography. Lane 1) 30% amplitude lysate. Lane 2) 30% amplitude flow through. Lane 3) 30% amplitude eluate; Lane 4: 30% amplitude NaCl flow through #1. Lane 5) 30% amplitude NaCl flow through #2. Lane 6) 2.5 minute lysate. Lane 7) 2.5 minute flow-through. Lane 8) 2.5 minute eluate. **B)** Coomassie blue stained protein gel after affinity chromatography. **C)** Western blot analysis using anti-GPSM2 primary antibody after affinity chromatography. **B&C)** Lane 1) Lysate of 2.5 minutes and 40% amplitude, Lane 2) Lysate of 2.5 minutes and 50% amplitude, Lane 3) Lysate of 3 minutes and 50% amplitude, Lane 4) Eluate of 2.5 minutes and 40% amplitude, Lane 5) Eluate of 2.5 minutes and 50% amplitude, Lane 6) Eluate of 3 minutes and 40% amplitude, Lane 7) Eluate of 3 minutes and 50% amplitude.

Western blot analysis verified the presence of LGN when using the pET-15b—LGN vector (Figure 4A). In an attempt to increase the amount of protein being purified, multiple sonication conditions were tested. Sonication was performed at a reduced amplitude, 60% to 30%, or time, 5 minutes to 2.5 minutes. After one round of anion-exchange purification, a Western blot analysis showed that the sonication lasting 2.5 minutes resulted in the most LGN at 75 kDa compared to the sonication at 30% amplitude which displayed various sized fragments of LGN (Figure 5A), indicating that LGN is being degraded. Our results display that a shorter time of sonication at a higher amplitude is optimal for extracting LGN from the *E.*

coli cells without disrupting the integrity of the protein. Analysis of further experiments at 50% or 40% amplitude and 3 minutes or 2.5 minutes of sonication time were performed. A SDS-PAGE gel stained with coomassie blue showed various bands around 75 kDa where LGN is expected to be (Figure 5B). Detection of LGN through a Western blot analysis confirmed the presence of LGN (Figure 5C) but many bands were viewed throughout the membrane rather than just at 75 kDa. The presence of more bands in lanes 5, 6, and 7 compared to 4 after purification display degradation of the protein during sonication procedures of greater length or intensity. Upon further optimization of the sonication protocol, our results indicated the presence of LGN and showed that vigorous sonication can disrupt the stability of the structure of LGN protein. It has been determined that sonication conditions of 2.5 minutes and 40% amplitude provide the best ability to lyse the *E. coli* cells without disrupting the stability of the LGN protein.

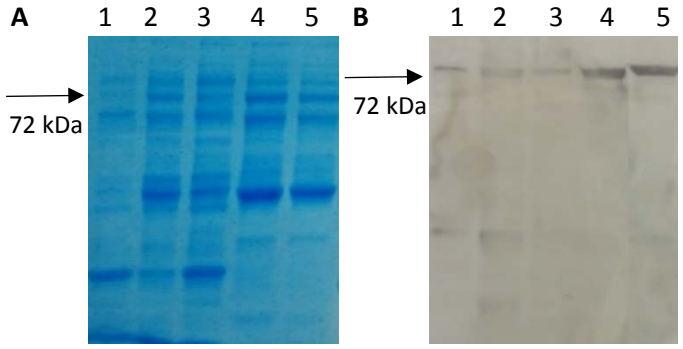

Figure 6: Analysis of buffer pH on LGN purification by anion-exchange chromatography by coomassie blue stained SDS-PAGE gel and Western blot. **A)** Coomassie blue stained protein gel after affinity chromatography. **B)** Western blot analysis using anti-GPSM2 primary antibody after affinity chromatography. **A&B)** Lane 1) Flow through using pH 8.0 buffer, Lane 2) Eluate using pH 8.0 buffer, Lane 3) Flow through using pH 7.7 buffer, Lane 4) Eluate using pH 7.7, Lane 5) Eluate using pH 6.8

Next, the binding and elution buffer pH effects on LGN purification were examined and compared to previous results at pH 7.3. Binding and elution buffers of pH 6.8, 7.7, and 8.0 were utilized to run the lysate and elute the protein from the anion-exchange column. After one round of anion-exchange purification at the various buffer pH values a coomassie blue stained gel showed similar protein samples were detected in lanes 2 through 5 at 75 kDa (Figure 6A). However, Western blot analysis showed that only lanes 4 and 5 displayed distinct bands near 75 kDa to identify the presence of LGN (Figure 6B). Our results show that both pH 7.7 and 6.8 are effective at binding LGN to the column and properly eluting it with the elution buffer.

To try to increase protein expression we tested the induction of LGN overexpression using the pET-28a—LGN and pET-15b—LGN vectors with IPTG in *E. coli* cells. Cell cultures that were induced with IPTG to express LGN were compared to uninduced cultures. The supernatant of each sample was run on a SDS-PAGE gel and stained with coomassie blue. The gel shows similar amounts of protein expressed at 75 kDa by both the uninduced (Lanes 1 & 3) and induced (Lanes 2 & 4) pET-15b—LGN (Lanes 1 & 2) vector and pET-

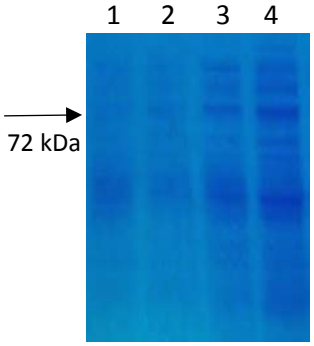

Figure 7: Analysis of IPTG on LGN expression in *E. coli* by coomassie blue stained SDS-PAGE gel. Lane 1) pET-15b—LGN uninduced, Lane 2) pET-15b—LGN induced, Lane 3) pET-28a—LGN uninduced, Lane 4) pET-28a—LGN induced.

28a—LGN (Lanes 3 & 4) vector (Figure 7). From these results we cannot confirm the overexpression of LGN by either the pET-28a—LGN or pET-15b—LGN vectors and we hypothesize the protein detected by the anti-GPSM2 antibody was a bacterial LGN homolog. Following these results, we decided to switch to a mammalian system and order the pCMV—LGN vector for LGN expression.

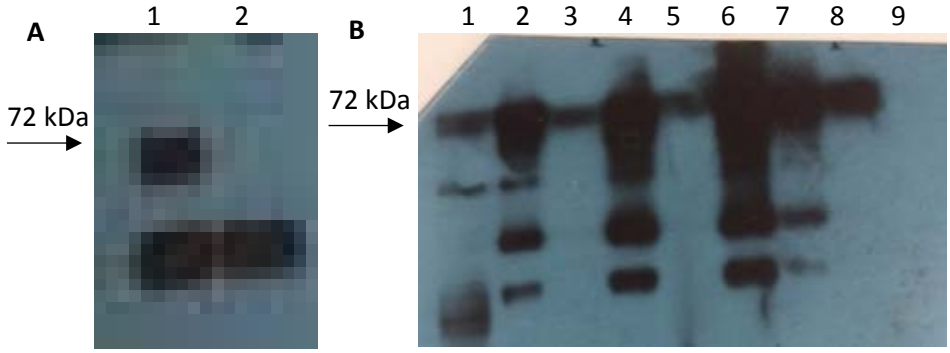

Figure 8: Western blots of LGN after immunoprecipitation using anti-GPMS2 antibody. **A)** Lane 1) Transfected BHK-570 immunoprecipitation, Lane 2) Untransfected BHK-570 immunoprecipitation. **B)** Immunoprecipitation was followed by peptide competition. Lane 1) Initial supernatant before peptide wash, Lane 2) Pellet from 1:1000 peptide wash, Lane 3) Supernatant from 1:1000 peptide wash, Lane 4) Pellet from 1:500 peptide wash, Lane 5) Supernatant from 1:500 peptide wash, Lane 6) Pellet from 1:100 peptide wash, Lane 7) Supernatant from 1:100 peptide wash, Lane 8) Pellet from wash without peptide, Lane 9) Supernatant from

Immunoprecipitation & Peptide Competition for LGN Purification

In order to successfully overexpress LGN, BHK-570 cells were transfected with pCMV—LGN and subsequently tested for overexpression of LGN protein. BHK-570 cells were chosen based on their natural expression of LGN which would suggest that overexpression of LGN would not damage the cells or interfere with their normal function. Immunoprecipitation was used as a method to isolate the LGN protein expressed in BHK-570 cells and analyzed through Western blotting. The results show that LGN was effectively expressed in BHK-570 cells and isolated by the immunoprecipitation, by the presence of a band at 75 kDa in lane 1 (Figure 8A).

In order to purify LGN for crystallography purposes, LGN protein expressed in BHK-570 cells must be isolated from the cell lysate. Since the goal was to isolate LGN, the protein must be separated from the antibody in order to continue purification. The first method that was explored was performing an elution of the protein from the pellet by washing the immunoprecipitation product with a competing LGN peptide at varying concentrations. Samples were taken from the initial supernatant before peptide was added to test whether all of the LGN was binding to the beads, as well as from each supernatant and pellet sample after the peptide was incubated overnight with the agarose beads. Samples were run on SDS-PAGE gel and protein presence in each sample was analyzed by Western blot (Figure 8B). The band at 75 kDa revealed that the amount of anti-GPSM2 antibody used was not sufficient for binding to

all of the LGN extracted from the BHK-570 cells. Western blot analysis also did not show significant competition of the peptide to elute LGN into the supernatant at any concentration as shown by significant bands present in all pellet fractions (Lanes 2, 4, 6, and 8) and only minimal bands in all supernatant fractions (lanes 3, 5, 7, and 9). Peptide based elution of LGN from the anti-GPSM2 antibody was unsuccessful and further methods must be employed in order to isolate LGN protein from the immuno-precipitation product. Once a method to elute LGN from its antibody is determined, the purification protocol can be optimized to purify LGN to 95% so that crystallization conditions can be tested and subsequently protein X-ray crystallography can be performed to determine the 3D structure of LGN and its mutants.

LGN Localization in BHK-570

Analysis of LGN presence in BHK-570 was performed through cell imaging using fluorescence microscopy of fixed cells. Images display the presence and effective immunostaining of LGN as seen by the green staining in the cell which suggests effective expression of LGN in the BHK-570 cells (Figure 9A). Based on the normal staining of DAPI (blue), this method does not interfere with cell viability and this system can be used an as effective method to study the localization of patterns of LGN and its mutants throughout the cell cycle, during specific stages of mitosis, and its interactions with other proteins. Next, the localization patterns of LGN expressed through the pCMV—LGN vector in BHK-570 cells were identified using fluorescence microscopy (Figure 9B). In BHK-570 cells, LGN (green) was detected throughout the cytosol as well as concentrating to the cell cortex (bright green dots). Our analysis of the localization patterns of wild-type LGN protein were consistent with localization patterns of associated proteins such as Ric-8a (29) indicating that LGN is functioning properly in BHK-570 cells. Further microscopic experiments must be performed including identifying LGN localization through the phases of mitosis as well as LGN localization coupled with localization of associated proteins and molecules. These experiments will allow us to understand the functions of LGN and when coupled with immunofluorescence experiments with the T450 mutants of LGN, we can interpret the effects of the T450 phosphorylation on LGN function and activity.

The expression levels of LGN by the pCMV—LGN vector in BHK-570 cells compared to amount of endogenous LGN were tested. Immunofluorescence of untransfected BHK-570 cells (Figure 9C) was compared to transfected cells (Figure 9D). Cells imaging revealed that minimal overexpression of LGN occurred in the BHK-570 cells. Although the microscopy reveals that a few cells may be overexpressing LGN (faint green), it cannot be concluded that overexpression is occurring due to the pCMV—LGN vector. Next, an alternate test of expression of LGN by the pCMV—LGN vector in BHK-570 cells was performed. An immunoprecipitation of untransfected BHK-570 cells was compared to transfected cells. Western blot analysis showed undesirable results because a significantly higher amount of LGN was expected in lanes 6-11, especially in lanes 8 and 10 where the LGN remained in the pellet fraction (Figure 9E). Based on the results from both the microscopy and immunoprecipitation, overexpression is not reliably occurring and the LGN detected in previous experiments was most likely endogenous LGN rather than the protein expressed through the pCMV—LGN vector. The initial immunoprecipitation results (Figure 8A) reveal that LGN expression in BHK-570 cells is possible and later attempts to transfect the cells could have been unsuccessful due to old reagents used in the transfection protocol. Furthermore, the Western blot detection is significantly more sensitive in detecting LGN than

immunofluorescence. The efficiency of the transfection protocol needs to be optimized in order to consistently achieve adequate overexpression of LGN by the pCMV-LGN vector.

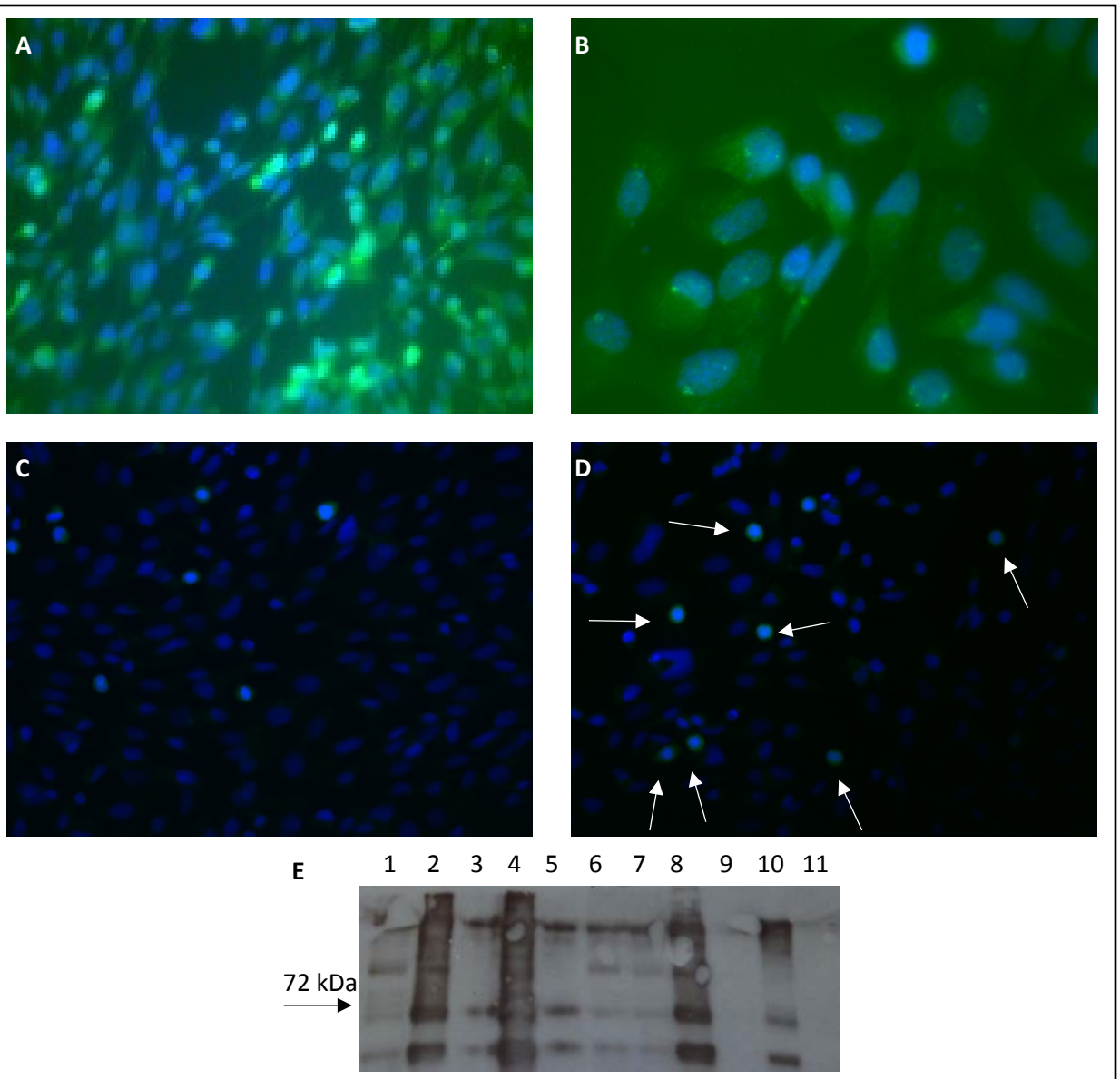

Figure 9: Analysis of LGN expression in BHK-570 cells by immunofluorescence and Western blot. **A,B,C,&D)** Fluorescent microscopy of LGN and nuclei in BHK-570 cells. Green fluorescence indicates the presence of LGN while blue fluorescence designates DNA. **A)** Transfected at 40x, **B)** Transfected at 100x, **C)** Untransfected at 40x, **D)** Transfected at 40x; possible overexpression is indicated by a faint green color and arrows, **E)** Western blot analysis using anti-GPSM2 primary antibody. Lane 1) Untransfected supernatant before wash, Lane 2) Untransfected pellet 1, Lane 3) Untransfected supernatant 1, Lane 4) Untransfected pellet 2, Lane 5) Untransfected supernatant 2, Lane 6&7) Transfected supernatant before wash, Lane 8) Transfected pellet 1, Lane 9) Transfected supernatant 1, Lane 10) Transfected pellet 2, Lane 11) Transfected supernatant 2.

T450 Mutagenesis

In order to generate the LGN mutations, PCR was used to perform Stratagene's QuikChange Site-Directed Mutagenesis on T450 in the LGN protein sequence in the pET-28a—LGN vector. When the mutated T450A plasmid was run on a 1% agarose gel, no band was present at 7.5 kb (Figure 10A). The negative results from our initial mutagenesis suggest that the plasmid was not present in the XL1-Blue supercompetent *E. coli* initially or could possibly be degraded during the mutagenesis process. In hopes of replicating the minimal PCR products, the PCR product was transformed into Top10 competent cells. Isolation of T450A pET-28a—LGN mutant plasmid and subsequent analysis on 1% agarose gel electrophoresis displayed faint bands at 3700 bp (data not shown). Subsequent attempts to maximize pET-28a—LGN mutagenesis product only resulted in what is most likely a portion of the initial vector which has been degraded or cleaved in vivo over time.

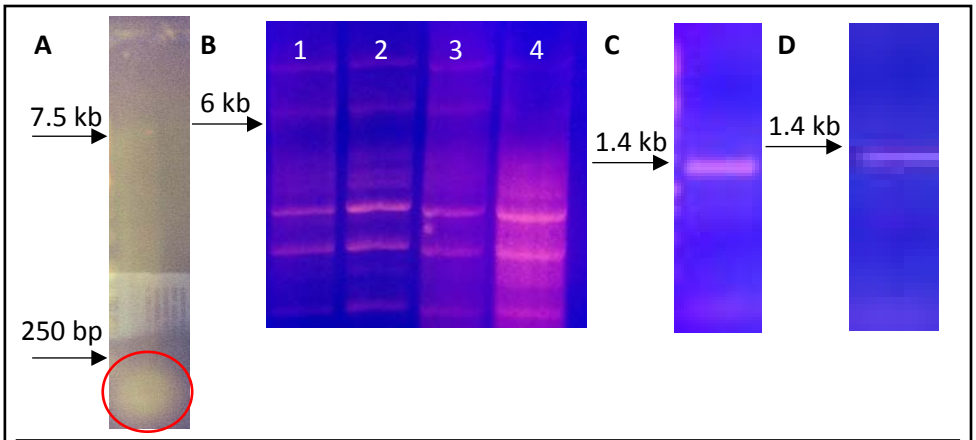

Figure 10: 1% agarose gels of PCR mutagenesis products. **A)** Isolated T450A plasmid from *E. coli* colony. DNA appeared at the bottom of the lane near 250 bp as indicated by the red circle. **B)** Lane 1) T450A mutagenesis with Agilent polymerase enzyme. Lane 2) T450A mutagenesis with Thermo Scientific Phusion polymerase enzyme. Lane 3) T450D mutagenesis with Agilent polymerase enzyme. Lane 4) T450D mutagenesis with Thermo Scientific Phusion polymerase enzyme. **C)** First T450A nested PCR product at 1.4 kb. **D)** First T450D nested PCR product at 1.4 kb.

With the switch to the mammalian expression system and pCMV—LGN vector we began site-directed mutagenesis with the new plasmid to produce T450A and T450D LGN. PCR products were transformed into DH5α cells, the cells were grown in culture, a mini-prep was performed, and products were run on a 1% agarose gel (data not shown). Only the T450D mutant products showed viable bands from the agarose gel electrophoresis. These products were sent to GENEWIZ for sequencing but the mutagenesis products that were able to be isolated from the agarose gel were not sufficiently pure to assess the sequence and confirm the mutation. The PCR reaction had to be refined in order to optimize product yield and generate a large, clean sample for sequencing. Again, site directed mutagenesis was performed to generate the T450A and T450D mutants. PCR products were run on a 1% agarose gel to analyze formation of a viable plasmid sample and to purify the sample for sequencing. Analysis of samples run on an agarose gel did not show significant bands at 6000 bp (Figure 10B), and the minimal bands present were not ample for sequencing. This further site-directed mutagenesis experimentation

did not improve the efficiency of the PCR. Thus, we switched to a different method to generate T450A and T450D mutants, nested PCR. Half of the first round of nested PCR was performed to generate one DNA segment of the LGN sequence to use as a template for subsequent PCR experiments to generate the full LGN mutants. This first round of PCR used T450A (Figure 10C) and T450D (Figure 10D) mutant primers to generate the latter half sequences and analysis of PCR products on a 1% agarose gel shows the expected products at 1400 bp. These will be used in further PCR experiments to generate the full length LGN coding sequence which then can be ligated into an empty pCMV expression vector for protein expression in vivo. After successful generation of the mutant pCMV—LGN plasmid it will be sent to GENEWIZ for sequencing to confirm the presence of the mutation.

Future Directions

Next, the second half of the first round of nested PCR will be performed in order to generate the second segment of LGN. Both segments from the first round will be used to perform the second round of nested PCR and generate the full-length LGN mutants which then can be ligated into a pCMV plasmid at the NotI sites. These mutant LGN plasmids can then be used to express forms of LGN which mimic unphosphorylated and phosphorylated LGN at T450.

Further experimentation must be performed in order to optimize BHK-570 transfection with pCMV—LGN. In order for transfection to be optimized, we must ensure that the cells are being properly maintained and well-nourished with growth media, the cells must be transfected at 75-80% confluency, and the proper amounts of liposomal reagent and plasmid are used for the transfection. Once optimal transfection efficiency is confirmed, overexpressed LGN in BHK-570 cells along with molecules that interact either directly or indirectly with LGN will be imaged using the immunofluorescence technique discussed previously. Possible immunofluorescence partners for LGN include but are not limited to $G_{\alpha i}$, NuMA, tubulin, dynein/dynactin, and F-Actin. Due to LGN's function occurring during mitosis, cell cycle arrest will be used to synchronize cell cycles by performing serum starvation, then serum will be added to the cell to release them for growth. Cells will be fixed during the various stages of mitosis to allow for localization of LGN in BHK-570 cells during specific phases of mitosis using immunofluorescence.

Immunofluorescence microscopy of LGN in conjunction with its direct or indirect binding partners to determine protein localization throughout the cell cycle will be performed. Comparing those results to the same experiments with T450A or T450D LGN can lead to an improved understanding of the effects of phosphorylation of T450 on LGN function. This understanding can lead to the development of breast cancer treatments which block the activation of LGN and prevent proliferation of cancer cells.

References:

1. Mochizuki, N; Cho, G; Wen, B; Insel, P. Identification and cDNA cloning of a novel human mosaic protein, LGN, based on interaction with $G_{\alpha i2}$. *Gene.* Online. **1996.** *181.* 39-43.

2. Du, Q.; Taylor, L.; Compton, D. A; Macara, I. G. LGN Blocks the Ability of NuMA to Bind and Stabilize Microtubules: A Mechanism for Mitotic Spindle Assembly Regulation. *Current Biology.* Online. **2002.** *12.* 1928-1933.

3. Pan, Z; Shang, Y; Jia, M; Zhang, L; Xia, C; Zhang, M; Wang, W; Wen, W. Structural and biochemical characterization of the interaction between LGN and Frmpd1. *Journal of Molecular Biology.* Online. **2013.** *425.* 1039-1049.

4. Bowman, S. K; Neumüller, R. A; Novatchkova, M.; Du, Q.; Knoblich, J. A. The Drosophila NuMA Homolog Mud Regulates Spindle Orientation in Asymmetric Cell Division. *Developmental Cell.* Online. **2006.** *10.* 731-742.

5. Mapelli, M.; Gonzalez, C. On the inscrutable role of Inscuteable: Structural basis and functional implications for the competitive binding of NuMA and Inscuteable to LGN. *Open Biology.* Online. **2012.** *2.* 120102.

6. McCudden, C. R; Willard, F. S; Kimple, R. J; Johnston, C. A; Hains, M. D; Jones. M. B; Siderovski, D. P. Gα selectivity and inhibitor of multiple GoLoco motif protein GPSM2/LGN. *Biochemica et Biophysica Acta.* Online. **2005.** *1745.* 254-264.

7. Spencer, J.; Darbyshire, K.; Boucher, A.; Kashem, M.; Long, L.; McGregor, I.; Karl, T.; and Arnold, J. Novel molecular changes induced by Nrg1 hypomorphism and Nrg1-cannabinoid interaction in adolescence: a hippocampal proteomic study in mice. *Front. Cell. Neurosci.* Online. **2013.** *7(15),* 1-13.

8. Blumer, J; Chandler, L; Lanier, S. Expression Analysis and Subcellular Distribution of the Two G-protein Regulators AGS3 and LGN Indicate Distinct Functionality. *Journal of Biological Chemistry.* Online. **2002.** *277:18.* 15897-15903.

9. Siller, K.; Doe, C. Spindle orientation during asymmetric cell division. *Nature Cell Biology.* Online. **2009.** *11,* 365-374.

10. Kimple, R.; Kimple, M.; Betts. L.; Sondek, J.; Siderovski, D. Structural determinants for GoLoco-induced inhibition of nucleotide release by Galpha subunits. *Nature*. Online. **2002.** *416,* 878–81.

11. Colombo, K.; Grill, W.; Kimple, R.; Willard, F.; Siderovski, D.; Gönczy, P. Translation of Polarity Cues into Asymmetric Spindle Positioning in *Caenorhabditis elegans* Embryos. *Science.* Online. **2003.** *300,* 1957-1961.

12. Zheng, Z.; Wan, Q.; Liu, J.; Zhu, H.; Chu X.; Du Q. Evidence for dynein and astral microtubule-mediated cortical release and transport of Gαi/LGN/NuMA complex in mitotic cells. *Mol Biol Cell.* Online. **2013.** *24:7,* 901-913.

13. Machicoane, M.; de Frutos, C. A.; Fink, J.; Rocancourt, M.; Lombardi, Y.; Garel, S.; Piel, M.; Echard, A. SLK-dependent activation of ERMs controls LGN–NuMA localization and spindle orientation. *J. Cell Biol.* Online. **2014.** *205,* 791-799.

14. Blumer, J. B; Kuriyama, R.; Gettys, T. W; Lanier, S. M. The G-protein regulatory (GPR) motif-containing Leu-Gly-Asn-enriched protein (LGN) and Giα3 influence cortical positioning of the mitotic spindle poles at metaphase in symmetrically dividing mammalian cells. *European Journal of Cell Biology.* Online. **2006.** *85.* 1233-1240.

15. Hao, Y; Du, Q; Chen, X; Zheng, Z; Balsbaugh, J; Maitra, S; Shabanowitz, J; Hunt, D; Macara, I. Par3 Controls Spindle Pole Orientation in Epithelial Cells by aPKC-Mediated Phosphorylation of Pins at the Apical Cortex. *Current Biology.* Online. **2010.** *20:20.* 1809-1818.

16. Compton, D.; Luo, C. Mutation of the predicted $p34^{cdc2}$ phosphorylation sites in NuMA impair the assembly of the mitotic spindle and block mitosis. *Journal of Cell Biology.* Online. **1995.** *108,* 621-633.

17. Zhu, J.; Wen, W.; Zheng, Z.; Shang, Y.; Wei, Z.; Xiao, Z.; Pan, Z.; Du, Q.; Wang, W.; Zhang, M. Structures of the LGN/mInsc and LGN/NuMA complexes suggest distinct functions of the Par3/mInsc/LGN and Gαi/LGN/NuMA pathways in asymmetric cell division. *Molecular Cell.* Online. **2011.** *43:3.* 418-431.

18. Du, Q.; Macara, I. Mammalian Pins Is a Conformational Switch that Links NuMA to Heterotrimeric G-Proteins. *Cell.* Online. **2004.** *119.* 503-516.

19. Du, Q.; Stukenberg, P.; Macara, I.A mammalian Partner of Inscuteable binds NuMA and regulates mitotic spindle organization. *Nature Cell Biology.* Online. **2001.** *12,* 1069-1075.

20. Gallini, S.; Carminati, M.; De Mattia, F.; Pirovano, L.; Martini, E.; Oldani, A.; Asteriti, I.; Guarguaglini, G.; Mapelli, M. NuMA Phosphorylation by Aurora-A Orchestrates Spindle Orientation. *Current Biology.* Online. **2016.** *26:4,* 458-469.

21. Matsumura, S; Hamasaki, M; Yamamoto, T; Ebisuya, M; Sato, M; Nishida, E; Toyoshima, F. ABL1 regulates spindle orientation in adherent cells and mammalian skin. *Nature Communications*. Online. **2012.** *3:626.* 1-10.

22. Lu, M.; and Johnston, C. Molecular pathways regulating mitotic spindle orientation in animal cells. *Development.* **2013.** *140*, 1843–1856.

23. Bergstralh, D.; and St Johnston, D. Spindle orientation: what if it goes wrong? *Semin. Cell Dev. Biol.* **2014.** *34*, 140–145.

24. Kozlowski, C.; Srayko, M.; Nedelec, F. Cortical microtubule contacts position the spindle in C. elegans embryos. *Cell*. **2007.** *129*, 499–510.

25. Kotak, S.; Busso, C.; Gönczy, P. Cortical dynein is critical for proper spindle positioning in human cells. *J Cell Biol*. **2012.** *199*, 97-110.

26. Gönczy, P.; Kotak, Sachin. Mechanisms of spindle positioning: Cortical force generators in the limelight. *Current Opinions in Cell Biology.* Online. **2013.** *25.* 741-748.

27. Fukukawa, C.; Ueda, K.; Nishidate, T.; Katagiri, T.; Nakamura, Y. Critical Roles of LGN/GPSM2 Phosphorylation by PBK/TOPK in Cell Division of Breast Cancer Cells. *Genes, Chromosomes & Cancer.* Online. **2010.** *49*, 861-872.

28. Tall, G; Gilman, A. Resistance to inhibitors of cholinesterase 8A catalyzes release of Gαi-GTP and nuclear mitotic apparatus protein (NuMA) from NuMA/LGN/Gαi-GDP complexes. *PNAS.* Online. **2005.** *102:46.* 16584-16589.

29. Woodard, G; Huang, N; Cho, H; Miki, T; Tall, G; Kehrl, J. Ric-8A and Giα Recruit LGN, NuMA, and Dynein to the Cell Cortex To Help Orient the Mitotic Spindle. *Molecular and Chemical Biology.* Online. **2010.** *30:14.* 3519-3530.

30. Pan, Z; Zhu, J; Shang, Y; Wei, Z; Jia, M; Xia, C; Wen, W; Wang, W; Zhang, M. An Autoinhibited conformation of LGN revels a distinct interaction mode between GoLoco motifs and TPR domains. *Structure.* Online. **2013.** *21.* 1007-1017.

31. Nipper, R. W; Siller. K. H; Smith, N. R; Doe, C. Q; Prehoda, K. E. Gαi generates multiple Pins activation states to link cortical polarity and spindle orientation in Drosophila neuroblasts. *PNAS.* Online. **2007.** *104.* 14306-14311.

32. Morin, X; Jaouen, F; Durbec, P. Control of planar divisions by the G-protein regulator LGN maintains progenitors in the chick neuroepithelium. *Nature Neuroscience.* Online. **2007.** *10:11.* 1440-1448.

Acknowledgments:

I would like to thank Dr. Brandy Sreenilayam for all of her guidance and encouragement throughout my time working with her and for the support in writing this thesis. Many thanks to all of the past and present students I have worked with on these projects; Autumn Smith, Adam Howard, Justin Galardi, Alexandra Rosekrans, Iliana Ruiz, Ayman Huzair, Stephen Valentino, and Icaro Alves-Pinto. I am also grateful to Dr. Laurie Cook for generously allowing us to utilize her laboratory facilities, teaching me the cell techniques, and all of her advice.

I am forever indebted to The College at Brockport for providing me with the opportunity to study and perform research through funding of the many research projects at Brockport. Specifically, I would like to thank the Department of Chemistry and Biochemistry, Department of Biology, and The Honors College for the opportunities to perform undergraduate research and compose an undergraduate research thesis. I would also like to thank the Institute of Engaged Learning and The Hallenbeck family for each providing me with the grants to perform research over the Summers of 2014 and 2015.